Axisymmetric lattice Boltzmann method

Jian Guo Zhou
Department of Engineering, University of Liverpool, Liverpool L69 3GQ, United Kingdom
(Received 15 February 2008; published 4 September 2008)

A lattice Boltzmann method is developed for incompressible axisymmetric flows. Both force and source or sink terms are incorporated into the lattice Boltzmann equation in a natural way, which is consistent in dimension with the lattice Boltzmann equation. The correct macroscopic equations for incompressible axisymmetric flows are recovered through the Chapman-Enskog expansion. It turns out that the added terms are nothing but the additional in the governing equations for the axisymmetric flows compared with the Navier-Stokes equations, resulting in a simple and efficient model. This provides an additional unique advantage that the proposed scheme is naturally suitable for general axisymmetric flows involving more physical phenomena. Two numerical simulations have been presented to verify the method.

DOI: 10.1103/PhysRevE.78.036701 PACS number(s): 47.11.−j

I. INTRODUCTION

It is not a dream but reality to simulate fluid flows with a simple arithmetic calculation instead of using the complicated flow equations. This is the basic idea behind the lattice Boltzmann method, which is characterized by a simple procedure, parallel process, and easy and efficient treatment of boundary conditions. The method has successfully been applied to different flow problems in science and engineering. Although it was originally developed to simulate fluid flows described by the Navier-Stokes equations, it has been improved and extended to other flow problems. For example, Swift *et al.* applied the lattice Boltzmann method to simulate nonideal fluids [1]. Spaid and Phelan, Jr. solved the Brinkman equation with the lattice Boltzmann method [2]. Zhou developed the lattice Boltzmann models for shallow water flows [3] and groundwater flows [4].

Axisymmetric flows represent numerous important flow problems in practice [5–9]. The three-dimensional (3D) lattice Boltzmann method has been applied to simulating 3D axisymmetric flows [10–12], in which the cubic lattices and a treatment of curved boundary are used. This implies that one or more dimensional lattices are required for simulation of the flows and hence the efficiency is reduced. Mathematically, 3D axisymmetric flows are effectively 2D problems in a cylindrical coordinate system. To make use of this feature, Halliday *et al.* [13] first studied the lattice Boltzmann method for axisymmetric flows in 2001. They introduced two source terms and recovered the macroscopic equations for the axisymmetric flows. The method of Halliday *et al.* has successfully been applied to a number of axisymmetric flow problems [5,6,14]. However, the one term in the momentum equation related to radial velocity is missed from the formulation of Halliday *et al.*, which causes large errors for axisymmetric flows with significant radial velocities in nonstraight pipes. This mistake is noticed and corrected by Lee *et al.* [15], demonstrating an accurate solution to flows when radial velocities cannot be ignored. In addition, the method of Halliday *et al.* has been extended to multiphase flow by Premnath and Abrahamand [7] and two phase flow with large density ratio by Shiladitya and Abraham [9]. Recently, following the similar idea to Halliday *et al.*, Reis and Phillips [8,16] modified the source terms in the approach of Halliday *et al.* in a slightly different manner without the mistake made by Halliday *et al.* The method was further successfully used for two numerical tests by the authors [17]. The main drawbacks of the existing methods are that the second source term involves more complicated terms than the original equations and the added forces cause inconsistency in dimension with the lattice Boltzmann equation.

Therefore in this paper, a simple and natural scheme is proposed to recover the macroscopic equations for the axisymmetric flows. The introduced source or sink and force terms in the method are just equivalent to the additional in the governing equations for the axisymmetric flows compared with the Navier-Stokes equations for incompressible flows, which is not only consistent in dimension with the lattice Boltzmann equation but also enables the present approach generally suitable for axisymmetric flows involving more physical phenomena. The new method has been applied to simulate two typical flows and the results are compared with analytical solutions, demonstrating its accuracy and applicability.

II. AXISYMMETRIC FLOW EQUATION

The governing equations for the incompressible axisymmetric flows in a cylindrical coordinate system can be written in tensor form as [18]

$$\frac{\partial u_j}{\partial x_j} = -\frac{u_r}{r}, \tag{1}$$

$$\frac{\partial u_i}{\partial t} + u_j \frac{\partial u_i}{\partial x_j} = -\frac{1}{\rho}\frac{\partial p}{\partial x_i} + \nu \frac{\partial^2 u_i}{\partial x_j^2} + \frac{\nu}{r}\frac{\partial u_i}{\partial r} - \frac{\nu u_i}{r^2}\delta_{ir}, \tag{2}$$

where ρ is the density, p is the pressure, t is the time, ν is the kinematic viscosity, i is the index standing for r or x, r and and x are the coordinates in radial and axial directions, respectively, u_i is the component of velocity in the i direction, δ_{ij} is the Kronecker delta function defined by

$$\delta_{ij} = \begin{cases} 0, & i \neq j, \\ 1, & i = j, \end{cases} \tag{3}$$

and the repeated indexes are the Einstein summation convention, which means a summation over the space coordinates. Such a convention is used throughout the paper without further indication.

Incorporation of the continuity equation (1) into the momentum equation (2) results in

$$\frac{\partial u_i}{\partial t} + \frac{\partial (u_i u_j)}{\partial x_j} = -\frac{1}{\rho}\frac{\partial p}{\partial x_i} + \nu \frac{\partial^2 u_i}{\partial x_j^2} - \frac{u_i u_r}{r} + \frac{\nu}{r}\frac{\partial u_i}{\partial r} - \frac{\nu u_i}{r^2}\delta_{ir}. \tag{4}$$

It may be pointed out that the third term on the right hand side of the above equation is missed in the method described by Halliday *et al.* [13].

III. LATTICE BOLTZMANN METHOD

A. Lattice Boltzmann equation

In order to simulate the axisymmetric flows, we propose the following general lattice Boltzmann equation with source or sink and force terms:

$$f_\alpha(\mathbf{x} + \mathbf{e}_\alpha \Delta t, t + \Delta t) - f_\alpha(\mathbf{x}, t) = -\frac{1}{\tau}(f_\alpha - f_\alpha^{eq}) + \theta \Delta t + \frac{\Delta t}{\mathcal{K} e^2} e_{\alpha i} F_i, \tag{5}$$

where f_α is the distribution function of particles, f_α^{eq} is the local equilibrium distribution function, Δt is the time step, $e = \Delta x / \Delta t$, Δx is the lattice size, τ is the single relaxation time [19], θ is a source or sink term that will be defined in Eq. (27) later, F_i is a force term that will be given by Eq. (47), and $\mathbf{x}$ is the space vector, i.e., $\mathbf{x} = (r, x)$, $e_{\alpha i}$ is the component of $\mathbf{e}_\alpha$, which is the velocity vector of a particle in the α link, and $\mathcal{K}$ is the constant defined by

$$\mathcal{K} = \frac{1}{e^2}\sum_\alpha e_{\alpha x} e_{\alpha x} = \frac{1}{e^2}\sum_\alpha e_{\alpha r} e_{\alpha r}. \tag{6}$$

In the present study, the nine-speed square lattice shown in Fig. 1 is used and $\mathbf{e}_\alpha$ is given by

$$\mathbf{e}_\alpha = \begin{cases} (0,0), & \alpha = 0, \\ \lambda_\alpha e \left[\cos \frac{(\alpha-1)\pi}{4}, \sin \frac{(\alpha-1)\pi}{4}\right], & \alpha \neq 0, \end{cases} \tag{7}$$

with λ_α defined as

$$\lambda_\alpha = \begin{cases} 1, & \alpha = 1,3,5,7, \\ \sqrt{2}, & \alpha = 2,4,6,8. \end{cases} \tag{8}$$

From Eq. (6), we have $\mathcal{K} = 6$.

The fluid density ρ and velocity u_i, are defined in terms of the distribution function as

$$\rho = \sum_\alpha f_\alpha, \quad u_i = \frac{1}{\rho}\sum_\alpha e_{\alpha i} f_\alpha. \tag{9}$$

The local equilibrium distribution function f_α^{eq} is

$$f_\alpha^{eq} = w_\alpha \rho \left(1 + 3\frac{e_{\alpha i} u_i}{e^2} + \frac{9}{2}\frac{e_{\alpha i} e_{\alpha j} u_i u_j}{e^4} - \frac{3}{2}\frac{u_i u_i}{e^2}\right), \tag{10}$$

which has the following properties:

$$\rho = \sum_\alpha f_\alpha^{eq}, \quad u_i = \frac{1}{\rho}\sum_\alpha e_{\alpha i} f_\alpha^{eq}, \tag{11}$$

where

$$w_\alpha = \begin{cases} \frac{4}{9}, & \alpha = 0, \\ \frac{1}{9}, & \alpha = 1,3,5,7, \\ \frac{1}{36}, & \alpha = 2,4,6,8. \end{cases} \tag{12}$$

B. Recovery of the axisymmetric flow equation

In this section, we perform the Chapman-Enskog expansion to show how the macroscopic equations (1) and (4) are derived from the lattice Boltzmann equation (5). For this, we assume that Δt is small and equal to ε,

$$\Delta t = \varepsilon. \tag{13}$$

Substitution of Eq. (13) into Eq. (5) leads to

$$f_\alpha(\mathbf{x} + \mathbf{e}_\alpha \varepsilon, t + \varepsilon) - f_\alpha(\mathbf{x}, t) = -\frac{1}{\tau}(f_\alpha - f_\alpha^{eq}) + \theta\varepsilon + \frac{\varepsilon}{6e^2} e_{\alpha i} F_i. \tag{14}$$

Taking a Taylor expansion to the left of Eq. (14) in time and space around point $(\mathbf{x}, t)$, we have

$$\varepsilon\left(\frac{\partial}{\partial t} + e_{\alpha j}\frac{\partial}{\partial x_j}\right) f_\alpha + \frac{1}{2}\varepsilon^2 \left(\frac{\partial}{\partial t} + e_{\alpha j}\frac{\partial}{\partial x_j}\right)^2 f_\alpha + \mathcal{O}(\varepsilon^3) = -\frac{1}{\tau}(f_\alpha - f_\alpha^{eq}) + \varepsilon\theta + \frac{\varepsilon}{6e^2} e_{\alpha i} F_i. \tag{15}$$

According to the Chapman-Enskog expansion, f_α can be written in a series of ε,

$$f_\alpha = f_\alpha^{(0)} + \varepsilon f_\alpha^{(1)} + \varepsilon^2 f_\alpha^{(2)} + \mathcal{O}(\varepsilon^3). \tag{16}$$

The centered scheme [20] is used for both source term θ and force term F_i as

$$\theta = \theta\left(\mathbf{x} + \frac{1}{2}\mathbf{e}_\alpha \varepsilon, t + \frac{1}{2}\varepsilon\right), \tag{17}$$

and

$$F_i = F_i\left(\mathbf{x} + \frac{1}{2}\mathbf{e}_\alpha \varepsilon, t + \frac{1}{2}\varepsilon\right), \tag{18}$$

which can also be written, via a Taylor expansion, as

$$\theta\left(\mathbf{x} + \frac{1}{2}\mathbf{e}_\alpha \varepsilon, t + \frac{1}{2}\varepsilon\right) = \theta + \varepsilon \frac{1}{2}\left(\frac{\partial}{\partial t} + e_{\alpha j}\frac{\partial}{\partial x_j}\right)\theta + \mathcal{O}(\varepsilon^2), \tag{19}$$

and

$$F_i\left(\mathbf{x}+\frac{1}{2}\mathbf{e}_\alpha\varepsilon,t+\frac{1}{2}\varepsilon\right)$$
$$=F_i(\mathbf{x},t)+\frac{1}{2}\varepsilon\left(\frac{\partial}{\partial t}+e_{\alpha j}\frac{\partial}{\partial x_j}\right)F_i(\mathbf{x},t)+\mathcal{O}(\varepsilon^2). \quad (20)$$

After substitution of Eqs. (16), (19), and (20) into Eq. (15), the equation to order ε^0 is

$$f_\alpha^{(0)}=f_\alpha^{eq}, \quad (21)$$

to order ε

$$\left(\frac{\partial}{\partial t}+e_{\alpha j}\frac{\partial}{\partial x_j}\right)f_\alpha^{(0)}=-\frac{1}{\tau}f_\alpha^{(1)}+\theta+\frac{1}{6e^2}e_{\alpha i}F_i, \quad (22)$$

and to order ε^2

$$\left(\frac{\partial}{\partial t}+e_{\alpha j}\frac{\partial}{\partial x_j}\right)f_\alpha^{(1)}+\frac{1}{2}\left(\frac{\partial}{\partial t}+e_{\alpha j}\frac{\partial}{\partial x_j}\right)^2 f_\alpha^{(0)}$$
$$=-\frac{1}{\tau}f_\alpha^{(2)}+\frac{1}{2}\left(\frac{\partial}{\partial t}+e_{\alpha j}\frac{\partial}{\partial x_j}\right)\theta+\frac{1}{12e^2}\left(\frac{\partial}{\partial t}+e_{\alpha j}\frac{\partial}{\partial x_j}\right)e_{\alpha i}F_i. \quad (23)$$

Using Eq. (22), we can write the above equation as

$$\left(1-\frac{1}{2\tau}\right)\left(\frac{\partial}{\partial t}+e_{\alpha j}\frac{\partial}{\partial x_j}\right)f_\alpha^{(1)}=-\frac{1}{\tau}f_\alpha^{(2)}. \quad (24)$$

From Eq. (22) + Eq. (24) $\times\varepsilon$, we have

$$\left(\frac{\partial}{\partial t}+e_{\alpha j}\frac{\partial}{\partial x_j}\right)f_\alpha^{(0)}+\varepsilon\left(1-\frac{1}{2\tau}\right)\left(\frac{\partial}{\partial t}+e_{\alpha j}\frac{\partial}{\partial x_j}\right)f_\alpha^{(1)}$$
$$=-\frac{1}{\tau}(f_\alpha^{(1)}+\varepsilon f_\alpha^{(2)})+\theta+\frac{1}{6e^2}e_{\alpha i}F_i. \quad (25)$$

Summation of the above equation over α provides

$$\frac{\partial}{\partial t}\left(\sum_\alpha f_\alpha^{(0)}\right)+\frac{\partial}{\partial x_j}\left(\sum_\alpha e_{\alpha j}f_\alpha^{(0)}\right)=9\theta. \quad (26)$$

Notice that Eq. (21) and substitution of Eq. (11) into the above equation result in the continuity equation (1), if the density variation is small enough and can be neglected, with θ defined by

$$\theta=-\frac{\rho}{9}\frac{u_r}{r}, \quad (27)$$

Taking $\Sigma e_{\alpha i}$ [Eq. (22) + $\varepsilon\times$ Eq. (24)] about α yields

$$\frac{\partial}{\partial t}\left(\sum_\alpha e_{\alpha i}f_\alpha^{(0)}\right)+\frac{\partial\Pi_{ij}^{(0)}}{\partial x_j}=\frac{\partial\Lambda_{ij}}{\partial x_j}+F_i, \quad (28)$$

where $\Pi_{ij}^{(0)}$ is the zeroth-order momentum flux tensor given by the following expression:

$$\Pi_{ij}^{(0)}=\sum_\alpha e_{\alpha i}e_{\alpha j}f_\alpha^{(0)}, \quad (29)$$

and

$$\Lambda_{ij}=-\frac{\varepsilon}{2\tau}(2\tau-1)\sum_\alpha e_{\alpha i}e_{\alpha j}f_\alpha^{(1)}. \quad (30)$$

Evaluating terms in Eq. (29) with Eq. (10), we have

$$\Pi_{ij}^{(0)}=p\delta_{ij}+\rho u_i u_j, \quad (31)$$

where $p=\rho e^2/3$ is the pressure, leading to a sound speed $C_s=e/\sqrt{3}$. Substitution of the above equation into Eq. (28) results in

$$\frac{\partial(\rho u_i)}{\partial t}+\frac{\partial(\rho u_i u_j)}{\partial x_j}=-\frac{\partial p}{\partial x_i}+\frac{\partial\Lambda_{ij}}{\partial x_j}+F_i. \quad (32)$$

Applying Eq. (22) we can rewrite Eq. (30) as

$$\Lambda_{ij}=\Pi_{ij}^{(1)}-\frac{\varepsilon}{2}(2\tau-1)\sum_\alpha e_{\alpha i}e_{\alpha j}\theta, \quad (33)$$

in which $\Pi_{ij}^{(1)}$ is the first-order momentum flux tensor,

$$\Pi_{ij}^{(1)}=\frac{\varepsilon}{2}(2\tau-1)\sum_\alpha e_{\alpha i}e_{\alpha j}\left[\left(\frac{\partial}{\partial t}+e_{\alpha k}\frac{\partial}{\partial x_k}\right)f_\alpha^{(0)}\right], \quad (34)$$

which can also be written with Eq. (29) as

$$\Pi_{ij}^{(1)}=\frac{\varepsilon}{2}(2\tau-1)\frac{\partial}{\partial t}\Pi_{ij}^{(0)}+\frac{\varepsilon}{2}(2\tau-1)\frac{\partial}{\partial x_k}\sum_\alpha e_{\alpha i}e_{\alpha j}e_{\alpha k}f_\alpha^{(0)}. \quad (35)$$

The second term in the above equation can be evaluated with Eqs. (10) and (21)

$$\frac{\partial}{\partial x_k}\sum_\alpha e_{\alpha i}e_{\alpha j}e_{\alpha k}f_\alpha^{(0)}=\frac{e^2}{3}\frac{\partial}{\partial x_k}(\rho u_i\delta_{jk}+\rho u_j\delta_{ki}+\rho u_k\delta_{ij}). \quad (36)$$

If we assume that characteristic velocity is U_c, length is L_c and time is t_c, we have that the term $(\partial/\partial t\Pi_{ij}^{(0)})$ is of order $\rho U_c^2/t_c$ and the term $(\partial/\partial x_k\Sigma_\alpha e_{\alpha i}e_{\alpha j}e_{\alpha k}f_\alpha^{(0)})$ is of order $\rho e^2 U_c/L_c$, based on which we obtain that the ratio of the former to the latter terms has the order

$$\mathcal{O}\left(\frac{\partial/\partial t\Pi_{ij}^{(0)}}{\partial/\partial x_k\Sigma_\alpha e_{\alpha i}e_{\alpha j}e_{\alpha k}f_\alpha^{(0)}}\right)=\mathcal{O}\left(\frac{\rho U_c^2/t_c}{\rho e^2 U_c/L_c}\right)=\mathcal{O}\left(\frac{U_c}{e}\right)^2$$
$$=\mathcal{O}\left(\frac{U_c}{C_s}\right)^2=\mathcal{O}(M^2), \quad (37)$$

in which $M=U_c/C_s$ is the Mach number. It follows that the first term in Eq. (35) is very small compared with the second term and can be neglected if $M\ll 1$; hence Eq. (35), after Eq. (36) is substituted, becomes

$$\Pi_{ij}^{(1)}=\frac{e^2\varepsilon}{6}(2\tau-1)\frac{\partial}{\partial x_k}(\rho u_i\delta_{jk}+\rho u_j\delta_{ki}+\rho u_k\delta_{ij}), \quad (38)$$

or

$$\Pi_{ij}^{(1)}=\nu\left[\frac{\partial(\rho u_i)}{\partial x_j}+\frac{\partial(\rho u_j)}{\partial x_i}+\frac{\partial(\rho u_k)}{\partial x_k}\delta_{ij}\right] \quad (39)$$

with the kinematic viscosity defined by

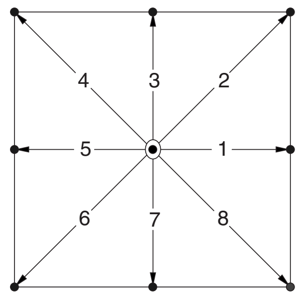

FIG. 1. Nine-speed square lattice.

$$\nu = \frac{e^2 \Delta t}{6}(2\tau - 1). \tag{40}$$

Inserting Eq. (39) into Eq. (33) and evaluating the rest terms of the equation, we obtain

$$\Lambda_{ij} = \nu \left[\frac{\partial(\rho u_i)}{\partial x_j} + \frac{\partial(\rho u_j)}{\partial x_i} + \frac{\partial(\rho u_k)}{\partial x_k}\delta_{ij} \right] - 18\nu\theta\delta_{ij}, \tag{41}$$

which is differentiated with respect to x_j, giving

$$\frac{\partial \Lambda_{ij}}{\partial x_j} = \nu \frac{\partial}{\partial x_j}\left[\frac{\partial(\rho u_i)}{\partial x_j} + \frac{\partial(\rho u_j)}{\partial x_i} + \frac{\partial(\rho u_k)}{\partial x_k}\delta_{ij} \right] - 18\nu \frac{\partial \theta}{\partial x_i}. \tag{42}$$

Substitution of Eq. (27) into the above equation leads to

$$\frac{\partial \Lambda_{ij}}{\partial x_j} = \nu \frac{\partial^2(\rho u_i)}{\partial x_j^2} + 2\nu \frac{\partial^2(\rho u_j)}{\partial x_i \partial x_j} + 2\nu \frac{\partial}{\partial x_i}\left(\frac{\rho u_r}{r}\right). \tag{43}$$

After applying the continuity equation (1), we have

$$\frac{\partial \Lambda_{ij}}{\partial x_j} = \nu \frac{\partial^2(\rho u_i)}{\partial x_j^2}. \tag{44}$$

Combining this with Eq. (32) results in

$$\frac{\partial(\rho u_i)}{\partial t} + \frac{\partial(\rho u_i u_j)}{\partial x_j} = -\frac{\partial p}{\partial x_i} + \nu \frac{\partial^2(\rho u_i)}{\partial x_j^2} + F_i. \tag{45}$$

Again, the density variation is assumed to be small enough, Eq. (45) can further be written as

$$\frac{\partial u_i}{\partial t} + \frac{\partial(u_i u_j)}{\partial x_j} = -\frac{1}{\rho}\frac{\partial p}{\partial x_i} + \nu \frac{\partial^2 u_i}{\partial x_j^2} + \frac{F_i}{\rho}. \tag{46}$$

Clearly, if we set

$$\frac{F_i}{\rho} = -\frac{u_i u_r}{r} + \frac{\nu}{r}\frac{\partial u_i}{\partial r} - \frac{\nu u_i}{r^2}\delta_{ir}, \tag{47}$$

Eq. (46) is just the momentum equation (4).

The calculation of F_i normally involves the velocity derivatives with respect to coordinate r. In order to find an efficient way in more consistent with the philosophy of the lattice Boltzmann method, we combine Eqs. (30) and (41) and have

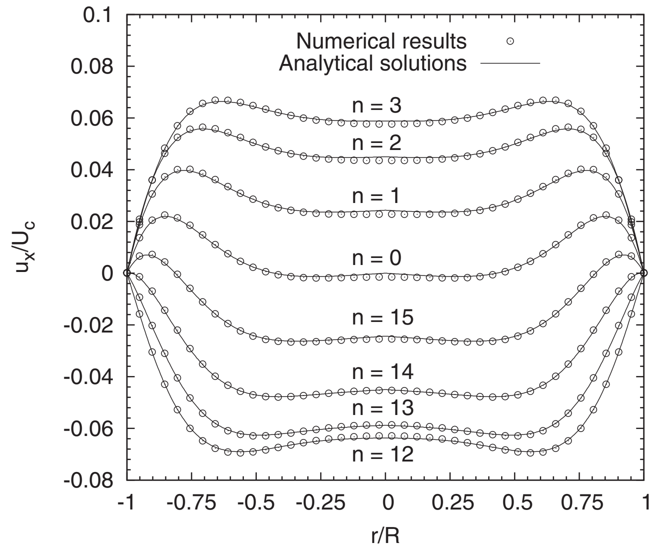

FIG. 2. Comparisons when u_x is increasing at different time $t = nT/16$ with $n = 0, 1, 2, 3, 12, 13, 14, 15$.

$$\nu \left[\frac{\partial(\rho u_i)}{\partial x_j} + \frac{\partial(\rho u_j)}{\partial x_i} + \frac{\partial(\rho u_k)}{\partial x_k}\delta_{ij} \right] - 18\nu\theta\delta_{ij} = -\frac{\varepsilon}{2\tau}(2\tau - 1)\sum_\alpha e_{\alpha i} e_{\alpha j} f_\alpha^{(1)}. \tag{48}$$

Rearranging Eq. (16) gives

$$f_\alpha^{(1)} = \frac{1}{\varepsilon}(f_\alpha - f_\alpha^{eq}) + \mathcal{O}(\varepsilon). \tag{49}$$

Applying this equation to Eq. (48) results in

$$\nu \left[\frac{\partial(\rho u_i)}{\partial x_j} + \frac{\partial(\rho u_j)}{\partial x_i} + \frac{\partial(\rho u_k)}{\partial x_k}\delta_{ij} \right] - 18\nu\theta\delta_{ij} = -\frac{2\tau - 1}{2\tau}\sum_\alpha e_{\alpha i} e_{\alpha j}(f_\alpha - f_\alpha^{eq}) + \mathcal{O}(\varepsilon^2). \tag{50}$$

The above equation can be used to evaluate

$$\frac{\partial u_x}{\partial r} = -\frac{3}{\rho \tau e^2 \Delta t}\sum_\alpha e_{\alpha x} e_{\alpha r}(f_\alpha - f_\alpha^{eq}) - \frac{\partial u_r}{\partial x} \tag{51}$$

and

$$\frac{\partial u_r}{\partial r} = -\frac{3}{2\rho \tau e^2 \Delta t}\sum_\alpha e_{\alpha r} e_{\alpha r}(f_\alpha - f_\alpha^{eq}) - \frac{1}{2}\frac{u_r}{r}, \tag{52}$$

reducing the calculations of the two derivatives $\partial u_x/\partial r$ and $\partial u_r/\partial r$ in Eq. (47) to one $\partial u_r/\partial x$ only, which can easily be determined with a finite difference scheme.

C. Features of the method

First of all, as seen from Eqs. (27) and (47), the added source or sink and force terms are just the additional in the governing equations for the axisymmetric flows compared with the Navier-Stokes equations for incompressible flows; hence it may be the simplest method. This is distinct from

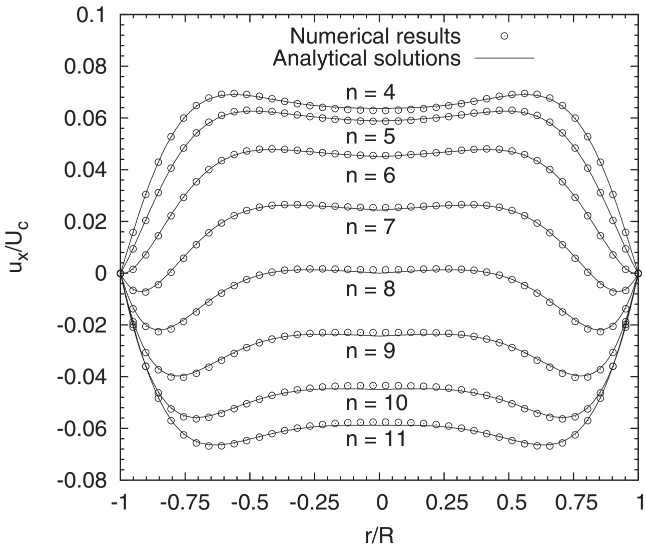

FIG. 3. Comparisons when u_x is decreasing at different time $t = nT/16$ with $n=4,5,6,7,8,9,10,11$.

the existing methods. In the method of Halliday *et al.* [13], the second force term has as many as five terms involving all the velocity derivatives with respect to both coordinates, which is more complicated than the original governing equations. Although the method is successfully applied to some axisymmetric flows [7,9,14], Lee *et al.* [15] have noticed that the term of $u_i u_r / r$ is missed in the method and shown that this term plays an important role in producing accurate solutions to axisymmetric flow problems with relatively larger radial velocity. They have then added the missing term in the method of Halliday *et al.* and demonstrated that the corrected force term can generate accurate solutions. As a result, the force contains more than ten terms, making the method more complex. Using the same idea of Halliday *et al.*, Reis and Phillips [8,16] provide the modified force, which also consists of more than ten terms.

Then, another feature is that the introduction of source or sink and force terms in the proposed method retains the consistency in dimension with the lattice Boltzmann equation (5). However, in the existing methods based on the approach of Halliday *et al.* the inclusion of force terms in that way inevitably leads to dimensional inconsistency in the lattice Boltzmann equation.

Finally, it is simple and straightforward to apply the present method to general axisymmetric flows which contain more additional terms than that given by Eqs. (1) and (4). For example, there are still additional external forces in the momentum equations for flow problems such as combustion. In this case, as long as the same additional terms are directly added in the expression (47) the proposed method will automatically recover the correct macroscopic equations without any further mathematical manipulation and can then be applied to solve the problem straightaway. On the other hand, to introduce an additional term like this for combustion in the existing methods will result in the force expressions to be derived again to recover the macroscopic equations, leading to more terms in the force expressions [15].

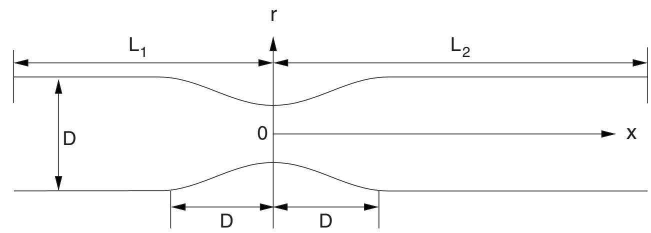

FIG. 4. Geometry of constricted pipe.

IV. NUMERICAL RESULTS

The method is applied to solve two flow problems, an unsteady Womersley flow and a steady flow through a pipe consisting of contraction followed by expansion. The results are compared with available analytical solutions. In the simulations, the bounce-back scheme is applied for no-slip boundary conditions along pipe walls. In addition, the lattice is arranged in such a way that the x axis is located both along the centerline of a pipe and in the middle of the two consecutive horizontal lattice lines in order to avoid the singularity at $r=0$ in the terms θ and F_i calculated from Eqs. (27) and (47), respectively. All the dimensional physical variables in SI units are used in the numerical computations.

A. 3D Womersley flow

The 3D Womersley flow or a pulsatile flow is an axisymmetric flow in a straight pipe. It is driven by a periodic pressure gradient at the inlet of the pipe and the pressure gradient is normally given by

$$\frac{dp}{dx} = p_0 \cos(\omega t), \tag{53}$$

where p_0 is the maximum amplitude of the pressure variation and $\omega=2\pi/T$ is the angular frequency, in which T is the period.

The Reynolds number is defined as $R_e=U_c D/\nu$ with the characteristic velocity U_c given by

$$U_c = \frac{p_0 \alpha^2}{4\omega\rho} = \frac{p_0 R^2}{4\rho\nu}, \tag{54}$$

in which $\alpha=R\sqrt{\omega/\nu}$ is the Womersley number, where R is the pipe radius and D is the diameter. The analytical solution for the velocity component in the axial direction for the Womersley flow is

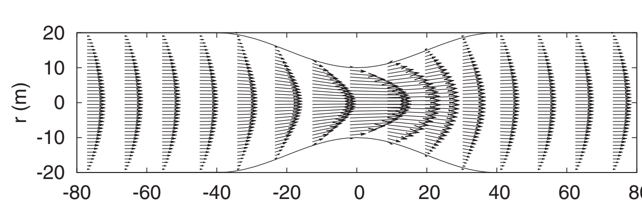

FIG. 5. Velocity vectors.

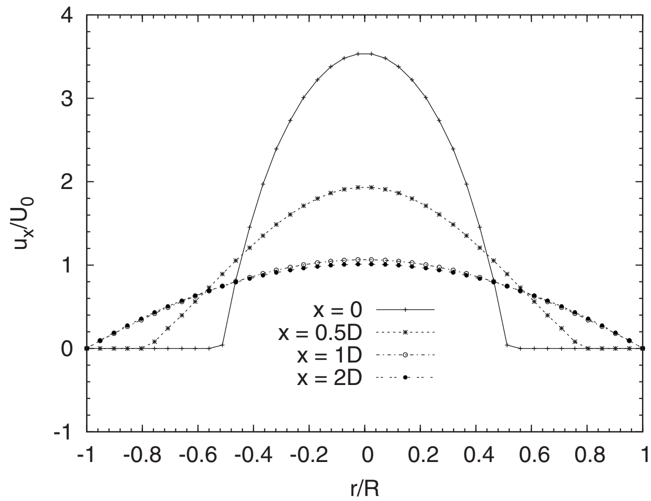

FIG. 6. Velocity u_x distribution across cross sections.

$$u_x(r,t) = \mathrm{Re}\left\{ \frac{p_0}{i\omega\rho}\left[1 - \frac{J_0(r\phi/R)}{J_0(\phi)} \right] e^{i\omega t} \right\}, \quad (55)$$

where J_0 is the zeroth order Bessel function of the first type, i is the imaginary unit, $\phi=(-\alpha+i\alpha)/\sqrt{2}$, and Re denotes the real part of a complex number.

The implementation of the periodic pressure gradient can be achieved by either applying an equivalent periodic body force [21] or specifying periodic pressure at the inlet and fixing the outlet pressure [22]. In the present study, the former is used, i.e., an additional body force is added to the existing force term F_i,

$$F_i = -\frac{\rho u_i u_r}{r} + \frac{\rho\nu}{r}\frac{\partial u_i}{\partial r} - \frac{\rho\nu u_i}{r^2}\delta_{ir} + p_0 \cos(\omega t)\delta_{ix}. \quad (56)$$

In the computation, $\rho=3$, $p_0=0.001$, $D=40$, $T=1200$, $\alpha=8$, $U_C=1$, which give $R_e=1200$. $\tau=0.6$ and 84×42 lattice are used in the simulation. The numerical solutions at different times are obtained after initial running time of $10T$. The corresponding results for velocity u_x are shown in Figs. 2 and 3, in which they are further compared with the analytical solution (55), showing good agreement.

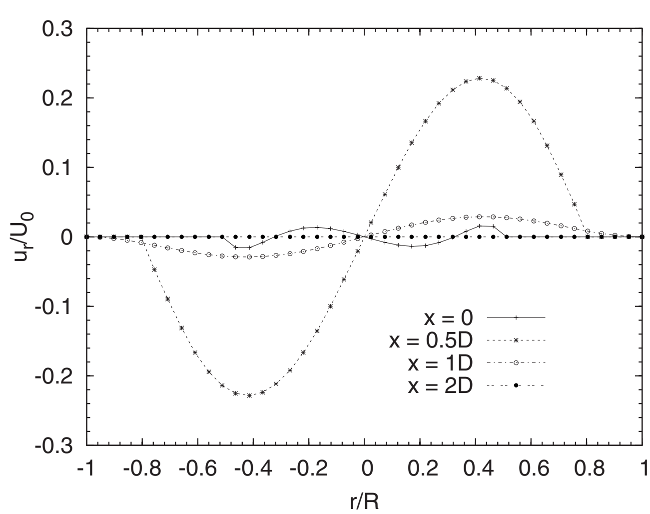

FIG. 7. Velocity u_r distribution across cross sections.

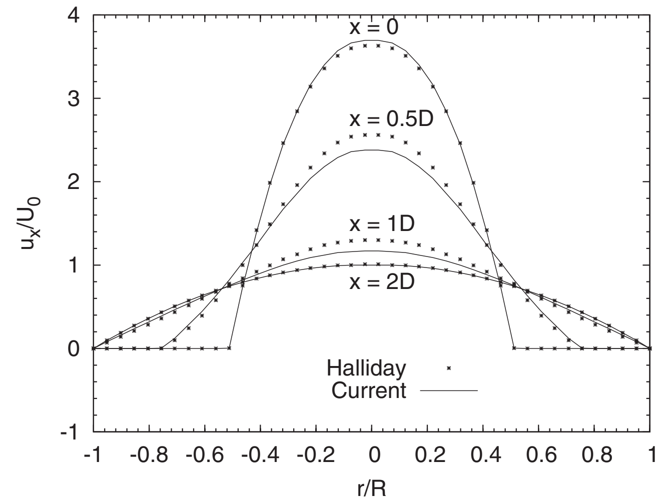

FIG. 8. Comparisons of velocity u_x with the method of Halliday *et al.* for $R_e=12.3$.

B. Steady flow through constricted pipe

We consider a steady flow through a constricted pipe with the diameter of $D=40$ m. The geometry of the pipe with the stenosis is described by the following function;

$$r(x) = R - \frac{0.5R[1+\cos(\pi x/D)]}{2}, \quad (-D < x < D), \quad (57)$$

and shown in Fig. 4, where $R=D/2$, $L_1=3D$, and $L_2=8D$.

In the numerical calculation, a parabolic profile for the velocity component u_x in the axial direction is specified at the inflow boundary,

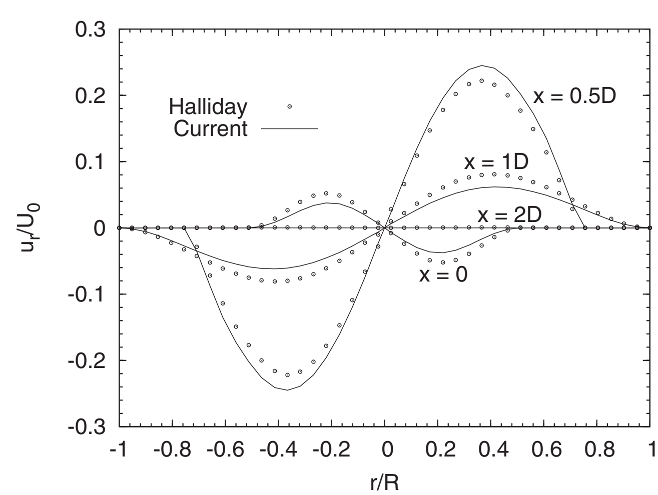

FIG. 9. Comparisons of velocity u_r with the method of Halliday *et al.* for $R_e=12.3$.

$$u_x = U_0\left[1 - \left(\frac{r}{R}\right)^2\right], \tag{58}$$

with $U_0 = 0.01$ m/s and the zero gradient for pressure is applied at the outlet boundary. 451×42 lattices are used with flow density of $\rho = 3$ kg/m^3. The Reynolds number is $R_e = 4.1$ ($R_e = U_0 D/\nu$). After the steady solution is reached, the velocity vectors are depicted in Fig. 5. The velocity profiles for two components u_x and u_r are shown in Figs. 6 and 7, respectively, which are in close agreement with that reported in the literature [15].

Finally, the proposed method is further tested with a larger Reynolds number, $R_e = 12.3$. The results are shown in Figs. 8 and 9 and compared with that by the method of Halliday *et al.* [13], showing that there is clear discrepancy between the results at positions where radial velocities are not small. In particular, the method of Halliday *et al.* underpredicts the velocity u_x at $x=0$, but overpredicts at $x=0.5D$ and $x=1D$. For velocity u_r, the method of Halliday *et al.* underpredicts at $x=0.5D$, but overpredicts at $x=0$ and $x=1D$. These findings are in good agreement with that reported by Lee *et al.* [15] and confirms that the missing term is important to produce accurate solutions to flows where the radial velocities cannot be neglected.

V. CONCLUSIONS

A simple lattice Boltzmann method for axisymmetric flows is presented. It is a natural and straightforward extension of that for Navier-Stokes equations. The introduction of the source or sink and force terms is consistent in dimension with the lattice Boltzmann equation. The added terms turn out to be the additional in the governing equations for the axisymmetric flows compared with the Navier-Stokes equations, leading to a general model for axisymmetric flows involving more physical phenomena. Its accuracy has been validated with two numerical tests. The model is able to predict steady and unsteady axisymmetric flows.

[1] M. R. Swift, W. R. Osborn, and J. M. Yeomans, Phys. Rev. Lett. **75**, 830 (1995).
[2] M. A. A. Spaid and F. R. Phelan, Jr., Phys. Fluids **9**, 2468 (1997).
[3] J. G. Zhou, Comput. Methods Appl. Mech. Eng. **191**, 3527 (2002).
[4] J. G. Zhou, Int. J. Mod. Phys. C **18**, 973 (2007).
[5] Y. Peng, C. Shu, Y. Chew, and J. Qiu, J. Comput. Phys. **186**, 295 (2003).
[6] X. D. Niu, C. Shu, and Y. T. Chew, Int. J. Mod. Phys. C **6**, 785 (2003).
[7] K. N. Premnath and J. Abraham, Phys. Rev. E **71**, 056706 (2005).
[8] T. Reis and T. N. Phillips, Phys. Rev. E **75**, 056703 (2007).
[9] S. Mukherjee and J. Abraham, Phys. Rev. E **75**, 026701 (2007).
[10] R. S. Maier, R. S. Bernard, and D. W. Grunau, Phys. Fluids **8**, 1788 (1996).
[11] R. Mei, W. Shyy, D. Yu, and L. S. Luo, J. Comput. Phys. **161**, 680 (2000).
[12] A. M. Artoli, A. G. Hoekstra, and P. M. A. Sloot, Int. J. Mod. Phys. C **13**, 1119 (2002).
[13] I. Halliday, L. A. Hammond, C. M. Care, K. Good, and A. Stevens, Phys. Rev. E **64**, 011208 (2001).
[14] T. S. Lee, H. Huang, and C. Shu, Int. J. Numer. Methods Fluids **49**, 99 (2005).
[15] T. S. Lee, H. Huang, and C. Shu, Int. J. Mod. Phys. C **17**, 645 (2006).
[16] T. Reis and T. N. Phillips, Phys. Rev. E **76**, 059902(E) (2007).
[17] T. Reis and T. N. Phillips, Phys. Rev. E **77**, 026703 (2008).
[18] L. D. Landau, *Fluid Mechanics*, 2nd ed. (Pergamon Press, Oxford, 1987).
[19] P. L. Bhatnagar, E. P. Gross, and M. Krook, Phys. Rev. **94**, 511 (1954).
[20] J. G. Zhou, *Lattice Boltzmann Methods for Shallow Water Flows* (Springer-Verlag, Berlin, 2004).
[21] J. A. Cosgrove, J. M. Buick, and S. J. Tonge, J. Phys. A **36**, 2609 (2003).
[22] X. He and L. Luo, J. Stat. Phys. **88**, 927 (1997).